

B. nonuniform axial heat flux treatment

BT data \Rightarrow $\begin{cases} \text{fluid} \\ \text{complex geometry} \\ \text{nonuniform axial and local heat flux} \end{cases}$

1. local cond. hypothesis

- : It is only the local heat and local quality that control the BT
- \therefore the upstream history is not important

2. Integral concept

- \rightarrow upstream history is quite important
 - \rightarrow strong dependence on axial heat flux profile
 - \rightarrow "upstream memory effect"
 - \rightarrow valid for the high quality condition

(A) F factor method : treat the effect of upstream history.

- : divide uniform axial CHF by upstream weighting factor, F, that yield the appropriate thermal limit for nonuniform axial heat flux profile.

$$\therefore F \equiv \frac{\overline{q_{\text{EO}}}}{q''_{\text{EO}}(L_{\text{eff}} + \lambda)} \quad \text{: Tong F factor} \quad (3.2.21)$$

$$= \frac{\Omega_{\text{eff}}}{q''_{\text{EO}}(L_{\text{eff}} + \lambda)[1 - e^{-\Omega_{\text{eff}}}]} \int_{\lambda}^{L_{\text{eff}} + \lambda} q''(g) \exp\{-\Omega_{\text{eff}}[(L_{\text{eff}} + \lambda) - g]\} dg$$

where $\Omega_{\text{eff}} = \frac{C}{D_{\text{eff}}} \approx \frac{0.135}{D_{\text{eff}}}$

As $\langle x_c \rangle_c$ increase, Ω_{eff} decrease.

★ Derivation of Tong F factor

- \rightarrow analyze the boiling crisis of non uniform heat flux distribution in a subcooled or low quality flow [Tong]
- : consider an overheating of surface due to a hot patch under bubble layer
 - $\left\{ \begin{array}{l} \text{big bubble at low flow rate and low pressure.} \\ \text{bubble layer at high flow rate and high pressure.} \end{array} \right.$

- o suggested the highly viscous bubble layer of crowded bubbles which covers a layer of superheated liquid near the wall
- o The liquid superheat and the local heat flux determine the wall temperature and thus the DNB condition.
- o In this model, the fluid enthalpy from an energy balance of the superheated liquid layer is a representative quantity for the onset of DNB

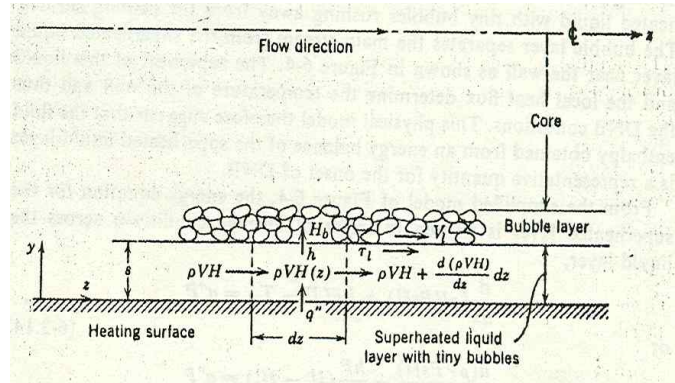


Fig. 3.1 Superheated liquid layer between bubble layer and heating surface

At low quality, the energy balance through the bubble layer is,

$$\begin{aligned} \frac{\partial}{\partial t} \left[\left(h - \frac{P}{\rho} \right) \rho P_H G \right] - z + H_{1\phi} (T - T_b) P_H - z + h G_c \Theta P_H \\ + \frac{\partial}{\partial z} [h G_c \Theta P_H] - z - h G_c \Theta P_H - q'' P_H - z = 0 \end{aligned}$$

Dividing $P_H - z$ and $T - T_b = \frac{1}{C_{pl}} [h - h_b]$

$$\therefore \frac{H_{1\phi}}{C_{pl}} (h - h_b) + \frac{\partial}{\partial z} [h G_c \Theta] - q'' + \frac{\partial}{\partial t} [h \rho \Theta - P \Theta] = 0$$

For steady state ($\frac{\partial}{\partial t} = 0$)

$$\frac{d}{dz} [h - h_b] + \Omega (h - h_b) = \Omega \frac{C_{pl}}{H_{1\phi}} q''$$

where $\Omega = \frac{H_{1\phi}}{G_c \Theta C_{pl}} = \frac{St}{\Theta} = const$

and $B, C = h(z - \lambda) - h_b - h$

Introducing the integrating factor, $e^{\Omega z}$,

$$(h(z) - h_b)_{non-uniform} = \frac{\Omega C_{pl}}{H_{1\phi}} \int_{\lambda}^z q''(z) e^{-\Omega(z - \lambda)} dz$$

For uniform axial heat flux,

$$(h(z) - h_s)_{\text{uniform}} = \frac{C_{\text{eff}} \bar{q}''}{H_{\text{eff}}} [1 - e^{-\Omega z}]$$

At the critical pt. (DNB), assume,

$$(h(z) - h_s)_{\text{nonuniform}} = (h(z) - h_s)_{\text{uniform}}$$

Then,

$$\bar{q}''_{\text{eff}(EQ)} = \frac{\Omega}{[1 - e^{-\Omega z_c}]} \int_{\lambda}^{z_c} q''(z) e^{-\Omega(z - z_c)} dz \quad (3.2.25)$$

: equivalent uniform axial CHF

Thus, Tong F factor will be

$$F \equiv \frac{\bar{q}''_{\text{eff}(EQ)}}{q''_c(Z_c)} = \frac{\Omega}{q''_c(Z_c) [1 - e^{-\Omega z_c}]} \int_0^{z_c} q''(z) e^{-\Omega(z_c - z)} dz$$

for nonuniform heat flux in PWR

Empirically,

$$\Omega = 0.44 \frac{[1 - x(Z_c)]^{7.23}}{(G/10^6)^{-1.72}} \quad [\text{in}^{-1}]$$

PWR : low quality \rightarrow high Ω

BWR : high quality \rightarrow low Ω

Consider $q''(z) e^{-\Omega(z_c - z)}$

a) For PWR having large Ω ,

Eq.(3.2.25) dies out,

\therefore little upstream "memory" effect

i.e. local heat flux is important

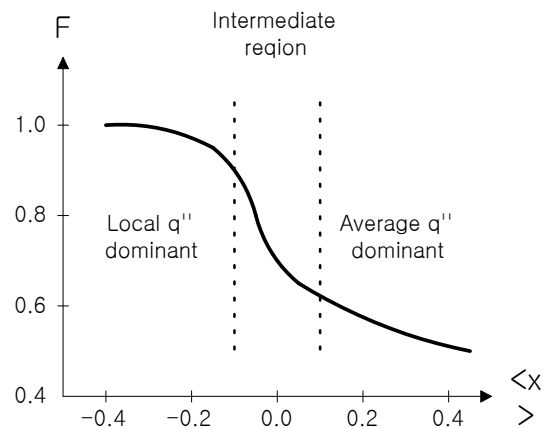
b) for BWR \rightarrow small Ω

\therefore upstream history is important ($\propto e^{-\Omega(z_c - z)}$ is large)

For the case of very small Ω ($\lim \Omega \rightarrow 0$), Eq. (3.2.25) will be

$$\lim_{\Omega \rightarrow 0} F = \frac{\bar{q}''_{\text{eff}(EQ)}}{q''_c(L_B + \lambda)} = \frac{\Omega}{q''_c(L_B + \lambda) L_B} \int_{\lambda}^{L_B + \lambda} q''(z) dz$$

where $\bar{q}''_{\text{eff}(EQ)} = \frac{1}{z_c} \int_0^{z_c} q''(z) dz$



■ Drawbacks of Tong F factor

- a) Computer based calculation are expressed (numerical integration of exponential integral)
- b) Complex graphic interpretation is required
($\dot{q}_c \propto$ inlet subcooling, axial heat flux profile)
- c) Exponential weighting of the upstream history is not nearly important for BWR (high quality)

(B) The critical quality boiling length ($\langle X_e \rangle_c = L_{fc}$) approach

CISE in Milan, Italy

Note: o local condition, hypothesis : $\ddot{q}_c \propto \langle X_e \rangle_c$

o Tong F factor : local parameter \rightarrow modification of $CHF_{uniform}$

o $\langle X_e \rangle_c = L_{fc}$ approach : $\langle X_e \rangle_c \rightarrow L_{fc}$

$$D - I + S = 0$$

$$GA_{x-s} [h_f + \langle X_e \rangle h_{fg}] - GA_{x-s} h_f - \int_{\lambda}^{L_{fc} - \lambda} P_{II} \ddot{q}(z) dz = 0$$

where λ is given as

$$\int_0^{\lambda} P_{II} \ddot{q}(z) dz = GA_{x-s} \Delta h_{sub}$$

CISE correlation

$$\langle X_e \rangle_c = \frac{a(p, G) L_{fc}}{b(p, G, D_{II}) + L_{fc}}$$

Since BT data, Fig 1-25, for uniform axial heat flux profiles are trended to be linear in the flux-quality plane,

$$\overline{\ddot{q}_c}'' = n(G, p) + m(G, p) \langle X_e \rangle_c$$

From

$$\overline{\ddot{q}_c}''_{CISE} = \frac{1}{L_{fc}} \int_{\lambda}^{L_{fc} - \lambda} \ddot{q}_c(z) dz \quad \text{and} \quad \langle X_e \rangle_c = \frac{\int_{\lambda}^{L_{fc} - \lambda} \ddot{q}(z) P_{II} dz}{GA_{x-s} h_{fg}}$$

we can obtain

$$\langle X_e \rangle_c = \frac{(n/m) L_{fc}}{[(GA_{x-s} h_{fg}) / (m P_{II}) + L_{fc}]}$$

Thus, if we can determine n, m for uniform heat flux, BT for nonuniform axial heat flux can be obtained

- inadequate for cases of extreme axial heat flux profile.
 - the ratio of peak to avg. axial flux for BWR is ≈ 2.0

3) Parametric effects on CHF

a) Inlet subcooling

linearly increases with the inlet subcooling

However, as G decreases, the effect becomes smaller and finally nearly no effect for the case of experiments at low p and G .

b) Mass flux, G

increases as G increases, but depends on the pressure

At low p , it exists a region where CHF doesn't increase as G increases

c) System pressure, p

At low G , CHF for fixed ΔT_{sub} increases as p increases until $p \approx 100$

but decreases from $p \approx 100$ bar

d) Tube diameter, D

increases as D increases due to decrease of ΔT_{sub}

Effect of D increases as the inlet subcooling increases

e) Heated length, L

decreases as L increases due to increase of ΔT_{sub}

f) Exit quality, x_{exit}

strongly depends on flow geometry and conditions

At low quality, the increase of ΔT_{sub} decreases CHF.

g) Surface roughness

no effect, but shift the boiling curve

h) Effect of Acceleration

- cause the fluctuations of void, the decrease of velocity and the variance of flow parameters

CHF decreases with increasing acceleration.

$$CHF' / CHF = (1 - a/g)^{-1}$$

$$CHF' / CHF = 1.0 - 0.5 * a/g$$

$$CHF' / CHF = 0.85$$

- heaving : When the marine heaves, the coolant flow velocity would decrease, and will bring down the CHF.
- listing : As the marine lists, the hot fluid will concentrate on the side of core and the adverse flow will take place near the side. Thus, the local values of CHF will decrease.

d) Other Parameters

- ◆ higher lateral crossflow increase
- ◆ mixing vane on spacer increase
- ◆ greater axial spacing increase
- ◆ axial offset

D) CHF correlations

5) Measurement of CHF

- a) measurement the temperature excursion with thermocouple
- b) Bridge circuit : local resistance increase due to temperature increase
- c) Infra red burnout detector

6) Improvement of CHF

a) For boiling in internal flow

1. Generation of Swirl Flow

- twisted tape (or ribbon) : Δp and thus pump capacity increase
Tokamak cooling
- ribbed tube

large once through boiler in fossil plant 에 사용. 100% enhancement

2. Increase of heat transfer area using fin

3. Increase of turbulence or surface roughness control

- helical equipment inside tube

b) For rod bundle

1. spacing of grid

regime	mechanism	CHF
general	enthalpy mixing increase and uniform flow distribution	increase
low : X'	scattering bubble near heated surface	increase
high : X''	break of liquid film	decrease

2. mixing vane

regime	mechanism	CHF
general	enhanced mixing	increase
low $\dot{m} \rightarrow$	scattering bubble near heated surface, centrifugal acceleration	increase
high $\dot{m} \rightarrow$	break of liquid film	decrease
	droplet displacement from channel center to wall	increase

c) For pool

- oxidation or selective fouling of the heated surface
- extended surface by fin
- volatile liquid additives
- rotation or vibration of heater
- fluid vibration
- use of electric fields
 - enhancement from several tens % to 200%

7) Design limit for CHF

- Condition I
 ● Condition II
 protection from DNB
- Condition III
- Condition IV
 some level of fuel damage is permissible

DNBR Limit :

$$\text{DNBR} = \frac{\dot{q}_{CHF}(\text{correlation})}{\dot{q}_{actual}}$$

The correlation for \dot{q}_{CHF} should have 95% probability with 95% confidence.

a) Establishment of CHF 상관식

1. perform multi rods CHF experiment
 : CHF data
 2. perform Subchannel Analysis
 : determine the local parameters
 3. Regression Analysis
 : establish CHF correlation as a function of key thermal hydraulic parameters
 - F factor to account the nonuniformity of heat flux
 - grid correlation for mixing vane grid
- ⇒ CHF(x, p, D_H, T_{in}, G) with 95% probability at 95% confidence level

b) Design limit for CHF correlations, MDNBR

- W-3 (W) MDNBR = 1.3
 - W-3 L grid MDNBR = 1.3 (11x14, 15x15)
 - W-3 R grid MDNBR = 1.3 (17x17)
- WRB, MDNBR = 1.19 for typical cell
 MDNBR = 1.17 for thimble cell
- B&W-2 MDNBR = 1.3
- CE-1 MDNBR = 1.19

c) reactor thermal hydraulic design

↳ assure that minimum DNBR keep above Design Limit DNBR during normal operation and anticipated transients

1) deterministic limit DNBR

↳ DNBR whose possibility is less than 5% \geq Design limit

↳ conservative input at core minimum DNBR calculation

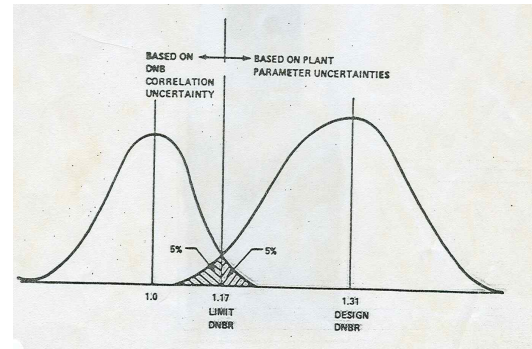
2) Statistical approach for limit DNBR

↳ Instead of using input parameters at their nominal or best estimate values,

↳ operating parameters

↳ nuclear and thermal parameters are considered statistical to obtain

↳ fuel fabrication parameters \rightarrow DNBR uncertainty factors



A. ITDP(Improved Thermal Design Procedure, Westinghouse)

B. Monte Carlo Method

(5) Post Boiling Transient Convective Heat Transfer

depends on the quality and flow rate at which BT occurs

1. for low quality-high flow BT

- o severe temperature excursion at DNB point
- o inverse annular flow

2. for high quality-low flow BT

- o milder temperature excursion
- o mist flow
- o typical in BWR technology

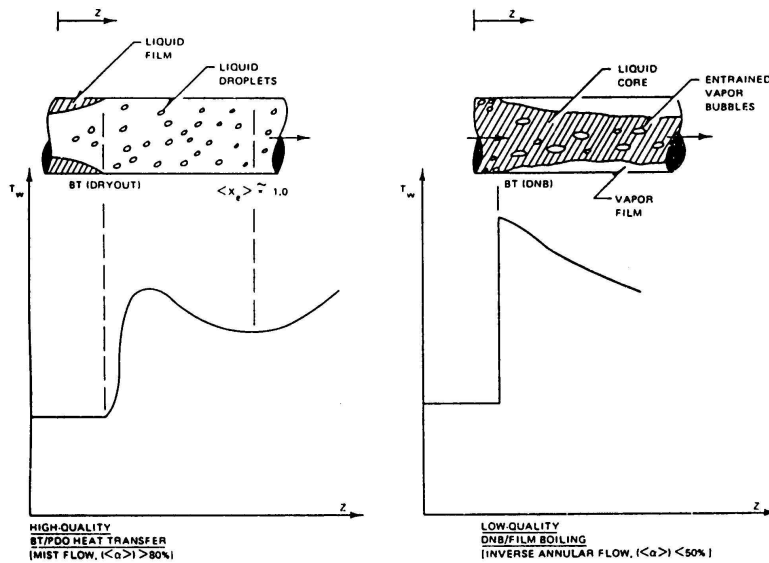
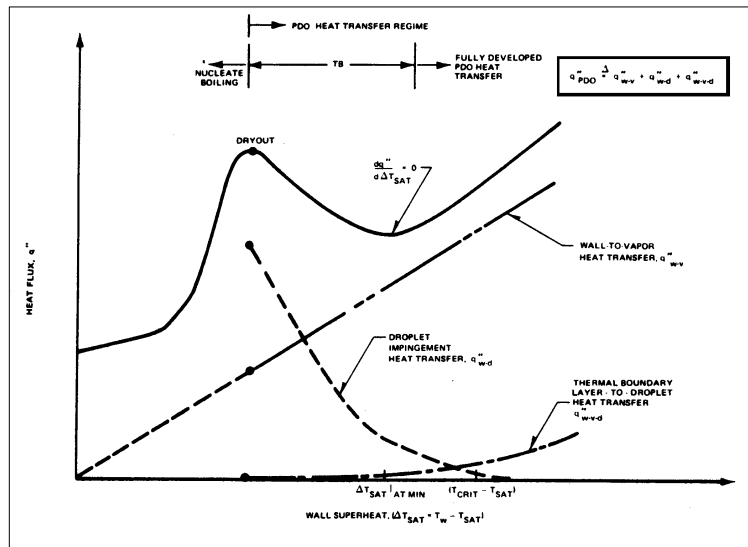


그림 1 Post-Boiling Transition Heat Transfer Regimes

1) Post-Dryout Mechanism



[14] A mechanistic Model of PDO Convective Heat Transfer

1. Wall → Vapor : heat transfer from surface to vapor under forced convection

- o thermal equilibrium model
- o frozen droplet model

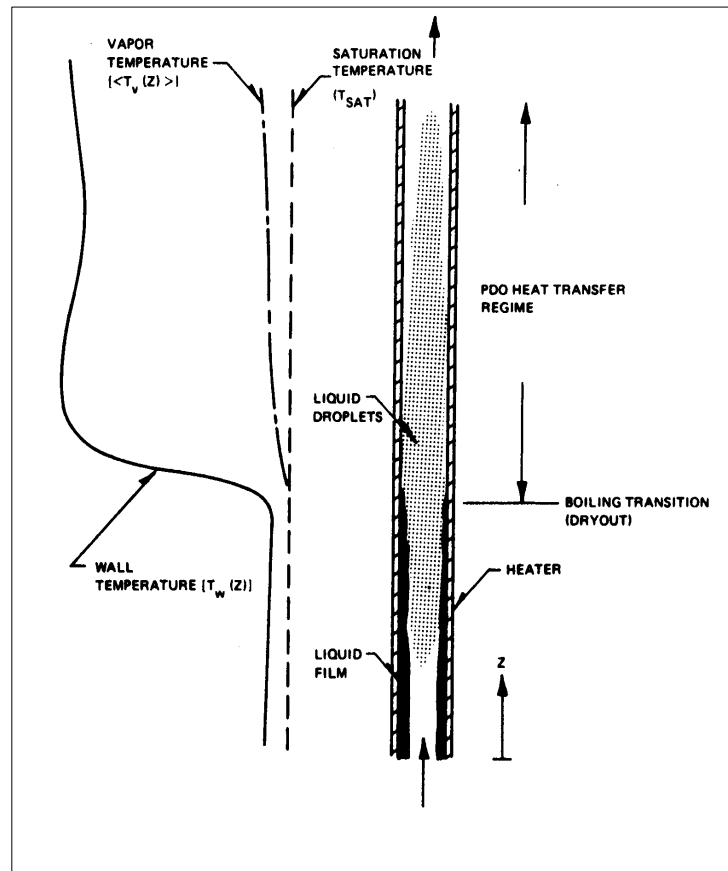
2. Wall → Droplet

Droplets fallen on the wall are evaporated if the wall temperature is not too high, and then cool the wall

3. Wall → Vapor → Droplet

At high surface temperature, droplets come close to the wall and enter the vapor surface layer. The side of droplets faces the high temperature of surface and so there is more evaporation on that side. This forces the droplet back from the surface.

2) PDO Heat Transfer Coefficient



- Determination of vapor temperature
important to determine PDO heat transfer coefficient

$$\dot{q}''_{PDO} = h_{PDO}(z) [T_s(z) - \langle T_v(z) \rangle]$$

Two bounding models

1) Thermal Equilibrium

Model

$$T_v = T_{SAT} = T_w(z) = T_{SAT}(z)$$

∴ no vapor superheat and all energy contribute only to evaporate droplets

2) Frozen Droplet Model

$$T_v(z) = T_{SAT}(z) + \Delta T$$

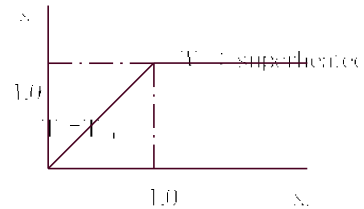
∴ no further liquid droplet evaporation, but superheating the vapor

► PDO heat transfer coefficient

For $\langle x_s \rangle \leq 1.0$ apply the thermal equilibrium model

$$N_{PDO}(z) = 0.023 \left[\frac{G \langle x(z) \rangle D_H}{\langle \alpha(z) \rangle \mu_c} \right]^{0.4} Pr_c^{0.4} Pr_f^{0.1}$$

• similar with Dittus-Boelter Eq



For $\langle x_s \rangle > 1.0$ apply the frozen droplet model

Here, the liquid droplets are assumed not to participate in the heat transfer process.

$$N_{frozen} = 0.023 \left[\frac{G \langle x(z) \rangle D_H}{\langle \alpha(z) \rangle \mu_c} \right]^{0.4} Pr_{frozen}^{0.4} \left(\frac{C_p^{liquid}}{C_p^{frozen}} \right)$$

• Global empirical correlations

- 1) Groeneveld correlation
- 2) Dougall-Rohsenow correlation
- 3) Bishop correlation for PWR

